

Article

Geospatial Assessment of Stormwater Harvesting Potential in Uganda's Cattle Corridor

Geoffrey Ssekyanzi^{1,2}, Mirza Junaid Ahmad³ and Kyung-Sook Choi^{3,4,*}

¹ Department of Food Security and Agricultural Development, Kyungpook National University, Daegu 41566, Republic of Korea; sskyanzigeoffrey11@gmail.com

² Department of Production, Rakai District Local Government, Kyotera P.O. Box 21, Uganda

³ Department of Agricultural Civil Engineering, Kyungpook National University, Daegu 41566, Republic of Korea; agri.junaid1205@gmail.com

⁴ Institute of Agricultural Sciences & Technology, Kyungpook National University, Daegu 41566, Republic of Korea

* Correspondence: ks.choi@knu.ac.kr; Tel.: +82-53-950-5731

Abstract: Freshwater scarcity remains a pressing global issue, exacerbated by inefficiencies in stormwater management during rainy seasons. Strategic stormwater harvesting offers a sustainable solution through runoff utilization for irrigation and livestock support. However, challenges such as limited farmer knowledge, difficult terrain, financial constraints, unpredictable weather, and scarce meteorological data hinder the accuracy of optimum stormwater harvesting sites. This study employs a GIS-based SCS-CN hydrological approach to address these issues, identifying suitable stormwater harvesting locations, estimating runoff volumes, and recommending site-specific storage structures. Using spatial datasets of daily rainfall (20 years), land use/land cover (LULC), digital elevation models (DEM), and soil data, the study evaluated 80 watersheds in Uganda's cattle corridor. Annual runoff estimates within watersheds ranged from 62 million to 557 million m³, with 56 watersheds (70%) identified for multiple interventions such as farm ponds, check dams, and gully plugs. These structures are designed to enhance stormwater harvesting and utilization, improving water availability for livestock and crop production in a region characterized by water scarcity and erratic rainfall. The findings provide practical solutions for sustainable water management in drought-prone areas with limited meteorological data. This approach can be scaled to similar regions to enhance resilience in water-scarce landscapes. By offering actionable insights, this research supports farmers and water authorities in effectively allocating stormwater resources and implementing tailored harvesting strategies to bolster agriculture and livestock production in Uganda's cattle corridor.

Academic Editor: Dharmappa Hagare

Received: 29 December 2024

Revised: 22 January 2025

Accepted: 23 January 2025

Published: 26 January 2025

Citation: Ssekyanzi, G.; Ahmad, M.J.; Choi, K.-S. Geospatial Assessment of Stormwater Harvesting Potential in Uganda's Cattle Corridor. *Water* **2025**, *17*, 349. <https://doi.org/10.3390/w17030349>

Copyright: © 2025 by the authors. Licensee MDPI, Basel, Switzerland. This article is an open access article distributed under the terms and conditions of the Creative Commons Attribution (CC BY) license (<https://creativecommons.org/licenses/by/4.0/>).

Keywords: stormwater harvesting; GIS; spatial data; SCS-CN; and Uganda's cattle corridor

1. Introduction

Freshwater scarcity, escalated by population growth, urbanization, and climate change, has intensified the global need for sustainable water management. With just 3% of the world's water being freshwater, pollution, exploitation, and the high costs of water extraction exacerbate the issue. In many African countries, these pressures are intertwined with poverty, hindering physical and economic water extraction, undermining community well-being [1–4]. Future predictions show the intensification of climate change

through increased occurrence of extreme events like floods and droughts [1,5,6]. This calls for sustainable water conservation solutions such as stormwater harvesting to minimize the environmental and social impacts of runoff and promote its utilization for essential activities like irrigation [7,8]. Sustainable solutions have stimulated increased research on stormwater harvesting in different aspects like structural designs, environmental implications, sustainable urban drainage designs, state-of-the-art perspective, and opportunities and challenges associated with stormwater harvesting [9–12]. Several factors limiting the widespread utilization of stormwater harvesting are sustainability, social and environmental, economic, and policy regulation issues [13]. These limit the adaptation and implementation strategies to solve stormwater challenges in developing countries [13]. Excess stormwater runoff causes erosion and flooding, damaging watersheds and resulting in loss of life and property. The development of strategies to capture and manage stormwater can reduce pressure on strained global water resources by providing sustainable alternatives to traditional water sources [14,15].

The process of identifying appropriate sites for stormwater harvesting involves ground footing to assess climate and hydrological parameters like rainfall patterns, topography, soil types, land use and land cover, environment, and socio-economic factors which requires time and often leads to delayed implementations [16–18]. Quantifying the amount of stormwater capture requires a solid understanding of rainfall-runoff dynamics with the watershed characteristics [19]. The relationship is significantly limited by station data deficiencies in areas with scarce and unreliable weather stations. Accessing accurate historical rainfall data is quite a challenge in the study area, posing great risks and inefficiencies in stormwater assessment [20–22]. Identifying suitable sites for stormwater harvesting in Uganda's cattle corridor faces numerous challenges which hampers the accuracy of hydrological assessments against climate alterations. Challenges including climate variability, where unpredictable rainfall patterns and irregular distribution can either exceed drainage capacities or lead to water shortages. Topographical and soil conditions, resource limitations, and socio-economic factors like land size and farmers' experience further hinder the adoption. Water quality issues from saline and agricultural runoff demand careful planning and, in some cases, require complex treatment solutions. Weak governance, inadequate infrastructure, limited financial and technical resources exacerbate these issues.

Uganda's economy relies on rainfed agriculture, accounting for 25% of the GDP, generating 35% of export revenue, and providing employment to 68% of the population [22]. Stormwater harvesting is instrumental in addressing water shortages in Uganda's cattle corridor to adapt to the unpredictable rainfall [23,24]. The region faces periodic droughts, making agricultural productivity vulnerable to recurrent crop failure and insufficient pasture for livestock, exacerbating poverty and food insecurity among rural households [22,25]. Implementing sustainable stormwater harvesting practices is vital to reduce the negative impacts of weather pattern destabilization in this critical economic sector [24,25]. Stormwater harvesting is a critical climate change adaptation strategy for supplementary irrigation to enhance crop productivity and livestock in the region [14,22]. Various stormwater harvesting technologies such as farm ponds, check dams and gully plugs are vital in combating water scarcity, augmenting agricultural output, and fortifying community resilience to unstable weather patterns.

This study focuses on optimizing stormwater harvesting in Uganda's cattle corridor by identifying suitable sites, estimating runoff volumes, and suggesting effective storage structures. We integrated spatial datasets such as rainfall, land use, soil types, and DEM within a GIS framework, to enhance the precision and efficiency of water capture. Remote sensing and satellite data address challenges like poor site selection and limited station data, ensuring more accurate watershed assessments [5]. With agriculture consuming 70%

of available water, the region's freshwater scarcity threatens livestock and crop productivity, highlighting the critical need for innovative stormwater storage solutions to bolster water security [26].

To combat water scarcity in agriculture and livestock during dry periods, governments and development partners promote adaptive strategies such as valley tanks, dams, and in situ stormwater harvesting techniques [21,27]. Widely adopted methods, including Fanya juu and Fanya chini trenches, enhance soil moisture, reduce erosion, and improve water infiltration, with around 66% of cattle keepers using smaller storage structures to increase water availability for agricultural needs [14,22,28,29]. Farmers rely on stormwater harvesting for livestock, household use, and micro-scale irrigation, with adoption shaped by factors like land size, herd size, experience, and group membership, where larger and more experienced farmers are the primary adopters [20,22,30]. However, the growing population and climate variability drive a rising demand for these technologies, emphasizing the urgent need for sustained investment and promotion to secure water access in the region [22].

This study adopts geospatial technologies like Arc GIS 10.7 software with the SCS-CN method to address data gaps, improve site selection accuracy, and optimize stormwater harvesting in Uganda's cattle corridor, where rainfall is unevenly distributed. The approach leverages spatial data on rainfall, land use, soil, and topography to estimate runoff and identify suitable harvesting sites, providing scalable, and cost-effective solutions for data-scarce regions [1,31–34]. GIS enhances runoff prediction by calculating weighted curve numbers, enabling temporal analysis, scenario modeling, and visual representation to support water management decisions [15,32,35–37]. The SCS-CN method, valued for its simplicity and minimal input requirements over other techniques like hydrograph analysis, rational method, computer simulation models, and hybrid techniques such as combining physically based and data driven approaches like Artificial Neural Networks, effectively estimates surface runoff by incorporating landscape and hydrological characteristics [6,8,32,34,38,39]. Combining this with satellite and remote sensing data offers near-real-time runoff estimates, crucial for ungauged watersheds [40]. By integrating technical, financial, and policy interventions, this approach strengthens farmers' resilience and promotes sustainable stormwater harvesting strategies, making it a reliable and scalable tool for water resource planning in data-limited environments.

2. Materials and Methods

2.1. Study Area Description

The study focused on 15 districts within Uganda's cattle corridor, covering an area of 29,567 km², located between 1° S to 1.5° N and 30° E to 33° E, represented by six traditional districts: Mbarara, Rakai, Sembabule, Kiboga, Mubende, and Luweero (Figure 1) [41]. Uganda's cattle corridor is a semi-arid region spanning over 40 districts, covering 84,000 km² occupying 43% of the country's total land area. It is dominated by savanna grasslands and drought-tolerant vegetation, serving as a pastoral and agricultural hub, producing over 95% of Uganda's beef [20,25,30]. However, it faces severe challenges due to erratic rainfall, frequent droughts, and water shortages, which hinder agricultural productivity and lead to significant crop losses [23,24]. The erratic and unevenly distributed rainfall (900–1500 mm annually), coupled with temperatures (21.5–30 °C), compounds the region's vulnerability to moisture stress and water scarcity [21,29,30]. Given its reliance on rainfed agriculture and limited groundwater resources, the area is highly suitable for exploring stormwater harvesting solutions to enhance agricultural resilience [23,24].

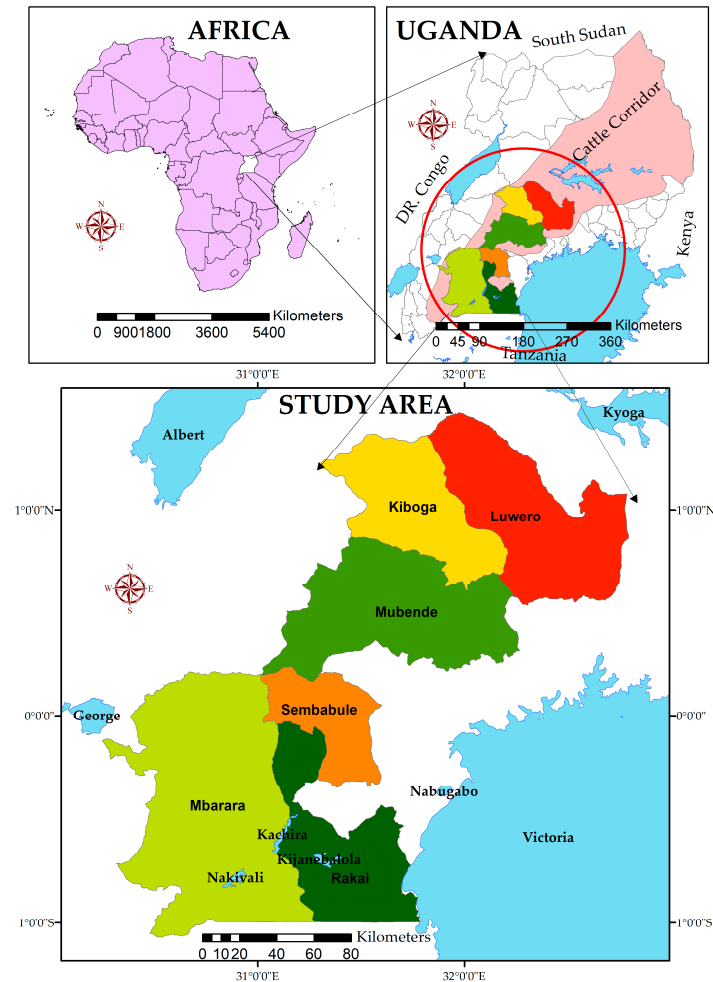


Figure 1. A map showing the study Area within the Uganda’s cattle corridor.

2.2. Data Sources

This study used diverse datasets, including Digital Elevation Models (DEM), land use/land cover (LULC), soil data, and rainfall records, sourced from reputable remote sensing platforms. The 30-m resolution DEM from USGS Earth Explorer was used to define watershed boundaries accurately [14,42]. LULC data for 2022 was sourced from MODIS MCD12Q1 V6.1 at a 500-m resolution. This dataset follows the IGBP classification standards provided by USGS Earth Explorer. Daily rainfall data (2004–2023) were sourced from PERSIANN through the CHRS portal, offering a detailed record of precipitation patterns at a $0.04^\circ \times 0.04^\circ$ spatial resolution [43]. Soil data from the FAO soil portal offered key insights into soil texture and hydrological soil groups (HSG) [18]. All data processing, analysis, and visualization were performed using ArcGIS 10.7 software.

2.3. Methodology

The study used the GIS-SCS-CN approach to assess stormwater runoff potential and determine the best sites and structures for storage (Figure 2) [18,35,39]. Key factors like LULC, slope, soil properties, stream order, and daily rainfall data were considered [7,18,33,44]. Rainfall, the primary driver of runoff, sets the thresholds for hydrological parameters, while LULC types like forests, croplands, and urban areas affect runoff conversion [5]. The DEM provides topographical details, highlighting slope and basin features that affect drainage and runoff patterns [18,45]. Steeper slopes lead to higher runoff, while flatter areas are more suitable for water harvesting [8,27,32,34]. Soil texture and HSG

classification determine infiltration rates, with poorly drained soils like clay generating more runoff [34,46]. The integration of these layers helps pinpoint ideal stormwater capture sites and structural designs for water scarcity solutions in Uganda’s cattle corridor [2,7,34,47].

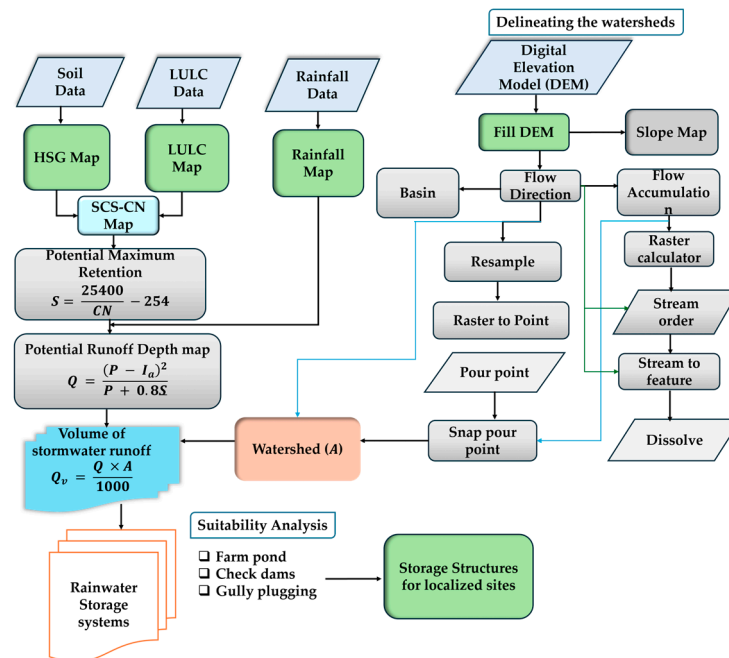


Figure 2. Schematic overview of the methodology.

2.3.1. Delineating Watersheds

Watershed delineation identifies drainage area boundaries and maps water flow through landscape features like valleys, ridges, and watercourses. It helps locate areas of water accumulation for hydrological analysis and assess the impact of land use on water resources. In this study, the DEM (Figure 3) was used as the base layer for flow analysis and was refined with ArcGIS hydrology tools, using the fill tool to correct imperfections and create a “filled” DEM [14,18,35]. The flow direction raster was derived to create the flow accumulation raster, which tracks the number of upslope cells contributing to each point on the landscape. High-flow areas were pinpointed by setting a threshold of 1200, highlighting cells with concentrated flow. A stream network was generated and classified into stream channels, and the flow accumulation zones were refined using zonal statistics and raster calculations to pinpoint cells with the highest accumulation [18,48].

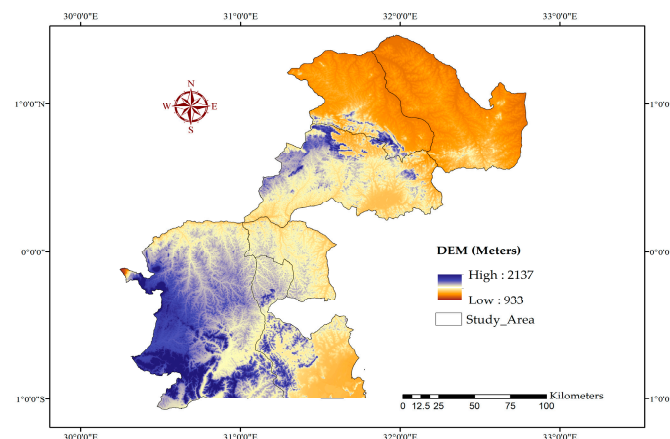


Figure 3. Study area DEM derived from the USGS earth explore.

Stream networks were analyzed and classified into six hierarchical classes using tools like stream order, stream-to-feature, and dissolve to examine tributary connections by grid code [49]. Flow directions were resampled for integration with spatial layers, and major basins feeding the streams were identified using the basin tool. The raster-to-point tool, based on the Eight Direction Pour Point model (Figure 4), assigned flow directions to watershed points for a detailed spatial analysis [18]. This converts the grid code points (Figure 4a) into corresponding angular flow directions (Figure 4b), effectively mapping the movement of water across the terrain.

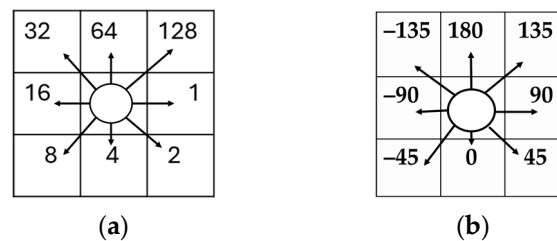


Figure 4. Eight Direction Pour Point model: (a) grid code values; (b) flow direction.

Small watersheds were delineated by manually selecting 80 pour points located at the outlets of level 3 tributaries [8,50] (Figure 5a). The Snap Pour Point tool accurately aligned these points with areas of highest flow accumulation [18]. The Watershed tool was used to define the upslope contributing areas for each pour point, creating a raster watersheds map consisting of 97 watersheds [32,47,50]. These were converted into vector format using the Raster to Polygon tool, generating 80 detailed small watershed boundaries (Figure 5b) [51]. Seventeen minor watersheds, which are less significant for runoff prediction and stormwater harvesting optimization, were excluded.

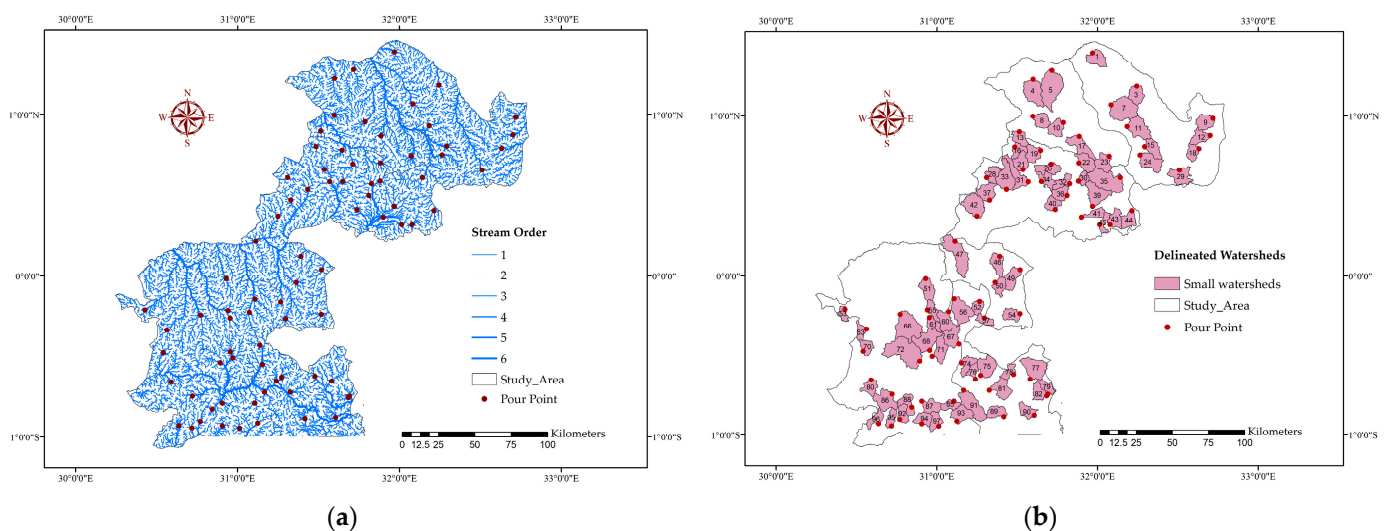


Figure 5. Mapping and defining the boundaries of drainage basins in the study area: (a) description of the stream segment classification based on grid code and location of the pour point; (b) demarcated watersheds and pour point.

2.3.2. Preparation of Layers for Stormwater Assessment

Thematic layers of LULC, soils, and rainfall were developed to aid in identifying areas with high flow accumulation and optimal stormwater capture potential [45,52]. GIS tools facilitated the preprocessing and reclassification of geographical, hydrogeological, and meteorological data, streamlining the selection of suitable harvesting sites [8]. MODIS land cover data was reclassified into five key LULC categories (Figure 6) by grouping

similar classes, such as merging forests and wetlands into broader categories like “Forest” and “Open Water”. Soil data were clipped and processed to create soil texture and HSG maps (Figure 7), highlighting infiltration and runoff characteristics [34]. Daily rainfall data from six weather stations (Mbarara, Mubende, Kiboga, Luweero, Rakai, and Sembabule), collected between 2004 and 2023, were interpolated using the Inverse Distance Weighted (IDW) method. This process generated 1682 point rainfall estimates (Figure 8a) and produced a high-resolution (0.040°) average annual rainfall map (Figure 8b) using the WGS UTM 36N projection, following Equation (1) [14,18].

$$P_{annual\ average} = \frac{(Raster\ 2004 + 2005 + 2006 + \dots + 2023)}{20} \quad (1)$$

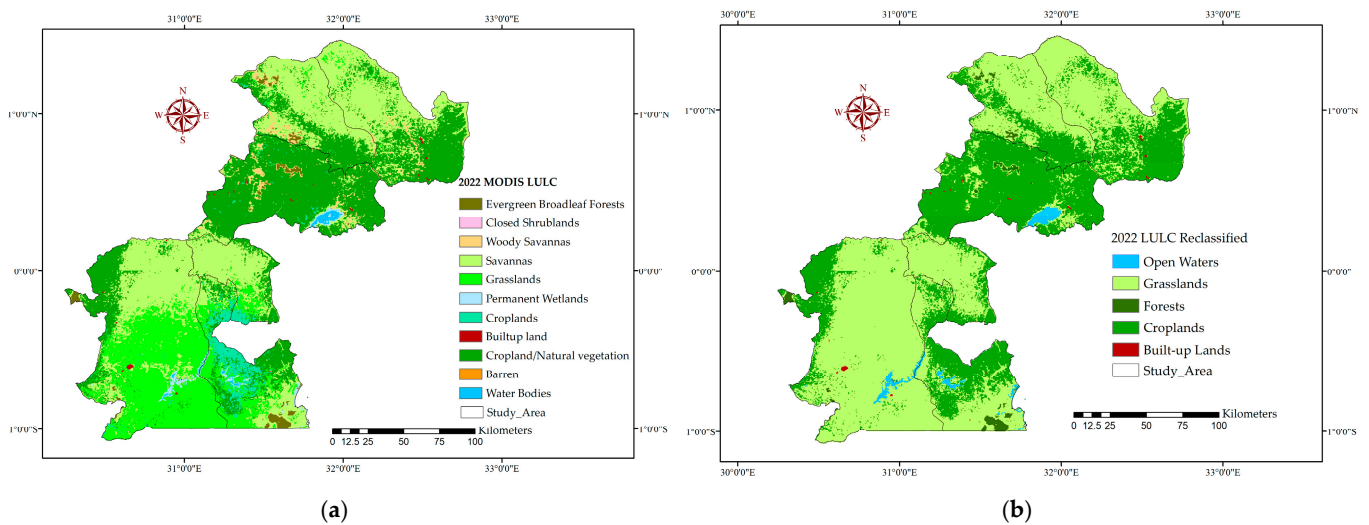


Figure 6. LULC categories in the study area: (a) MODIS land cover classification map; (b) map of the reclassified LULC.

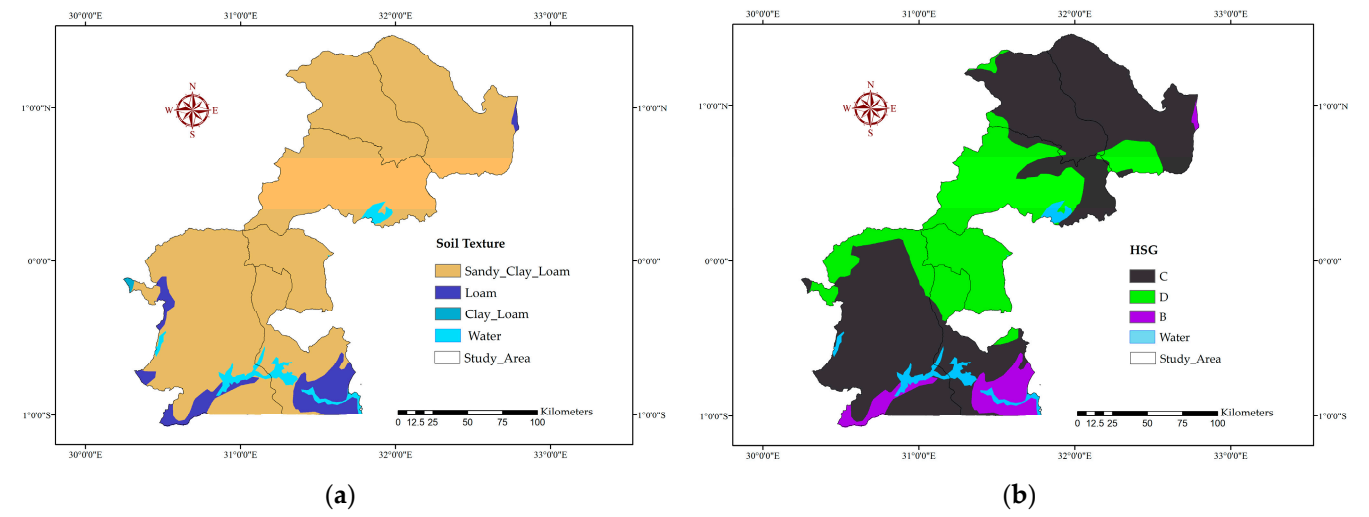


Figure 7. Maps describing the soil properties influencing stormwater harvesting site selection: (a) soil texture map; (b) HSG map.

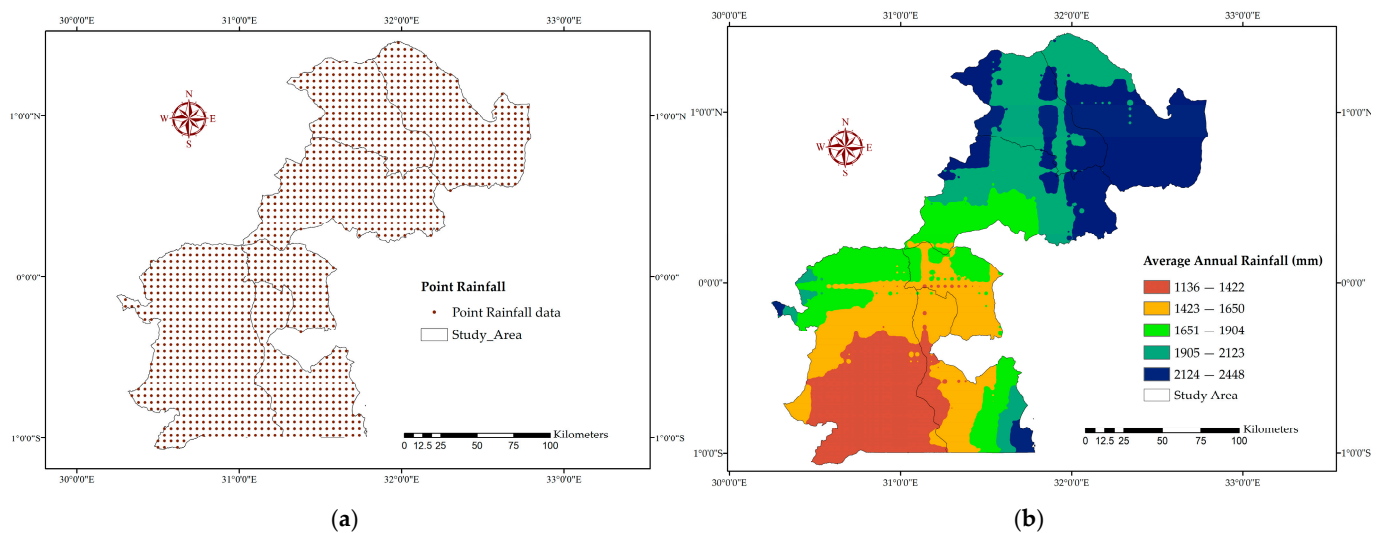


Figure 8. Rainfall distribution maps: (a) projected point rainfall distribution; (b) average annual rainfall distribution.

2.3.3. Surface Runoff Assessment Using the SCS-CN Technique

The USDA-developed SCS-CN method is a widely used approach for estimating surface runoff by encapsulating factors like soil properties, land use, and hydrological conditions into the CN, which represents a watershed’s rainfall (P) response (Equation (2)) [44]. Its integration with GIS enables precise spatial analysis and runoff mapping, making it effective for small watersheds (up to 250 km²) and adaptable for larger ones through CN adjustments [6,38]. Based on the hydrological balance equation, its simplicity, scalability, and minimal data requirements make it especially valuable in rural and data-scarce areas like the study region [1,6,8,53]. Designed for storm-specific scenarios, it has also been adapted to estimate annual runoff, offering a practical, versatile tool for water resource planning and sustainable management [6,8,34].

1. Soil analysis

Soils are classified into HSG A, B, C, and D, based on their infiltration capacity, with sandy soils having higher infiltration and low runoff. while clay soils generate more runoff due to lower infiltration rates [33,36]. The study soils were categorized into three HSG B, C, and D, primarily dominated by sandy clay loam texture, reflecting their varying infiltration capacity.

2. Land use land cover categories

LULC significantly influence runoff potential. Vegetated areas, such as forests or grasslands, enhance infiltration and reduce runoff, while impervious surfaces like roads and pavements increase runoff [2]. By combining LULC and HSG data, CN values were assigned to different zones (Table 1). Higher CN values closer to 100, indicate areas with high runoff and low infiltration, while lower CN values reflect better infiltration potential [2,8,31,44].

Table 1. CN values derived from LULC coverage matched with the HSG of the study area [44].

No.	LULC	Area (km ²)	Percentage (%)	HSG			
				A	B	C	D
1.	Grassland	18,995	58	—	69	79	84
2.	Cropland	12,704	39	—	78	85	89
3.	Open water	438	1	—	100	100	100
4.	Forests	341	1	—	55	70	77

5.	Built-up land	44	0	—	—	82	86
	Total	32,522	100				

The study accounted for antecedent moisture conditions (AMC) to reflect the soil moisture levels before rainfall that influence infiltration and runoff. AMC is classified into three levels: dry (AMC I), normal (AMC II), and wet (AMC III) [33,34,44,51,54]. For this analysis, CN values were selected based on normal moisture conditions (AMC II).

$$Q = \frac{(P - I_a)^2}{P + 0.8S} \tag{2}$$

The direct surface runoff (Q) is a function of precipitation (P), initial abstraction (I_a), and the potential maximum retention (S) after runoff begins. Initial abstraction represents a fraction of the potential retention given by Equation (3) [44,45].

$$I_a = \lambda \times S \tag{3}$$

where λ represents abstraction ratio, set at 0.2, based on the region’s seasonal water scarcity [3]. Although the area receives sufficient annual rainfall, water shortages occur during specific months, necessitating efficient stormwater harvesting and management.

Equations (2) and (3) constitute the core framework of the SCS-CN method, where initial abstraction accounts for interception, surface runoff, and infiltration prior to the onset of runoff. The potential maximum retention (S), derived from Equation (4), utilizes the CN values from the combination of LULC and HSG, representing the area’s runoff potential [8,44,45].

$$S = \frac{25400}{CN} - 254 \tag{4}$$

Equations (2)–(4) were integrated into GIS to generate spatial maps based on the CN values listed in Table 1. The resulting CN raster (Figure 9a) shows the spatial distribution of runoff coefficient with CN values ranging from 55 to 100. Using the CN raster and Raster Calculator, maps were generated to represent S (Figure 9b) and I_a , highlighting soil and land use water retention capacities. The retention map showed values ranging from 0 to 207 mm, with lower CN values indicating greater water retention potential compared to areas with higher CN values

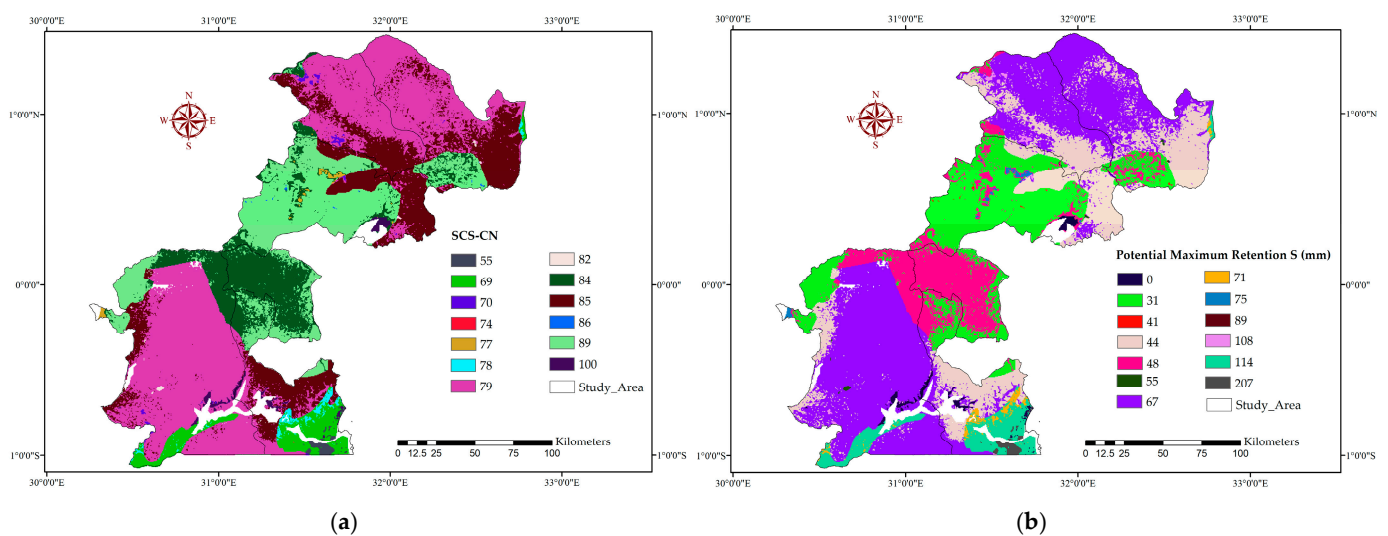


Figure 9. Schematic maps demonstrating the SCS-CN method. (a) CN map; (b) potential maximum retention (S) map.

2.3.4. Stormwater Runoff Volume Across Watershed

The stormwater runoff volume (Q_v) was calculated by multiplying the watershed area (A) with the runoff depth (Q) [32,47]. Watershed boundaries and runoff depth rasters, aligned within the same coordinate system, were used as the foundation. The Clip tool refined the runoff depth raster to fit watershed boundaries, and the Zonal Statistics as Table tool calculated the mean runoff depth (Q) for each watershed. Finally, the Field Calculator was used to compute the watershed runoff volume in cubic meters using Equation (5).

$$Q_v = \frac{Q \times A}{1000} \quad (5)$$

2.3.5. Determining Optimal Stormwater Storage Solutions for Selected Sites

Stormwater harvesting structures are vital for water conservation, especially when tailored to the watershed's unique attributes of topography and runoff volume [18,45]. Common structures like farm ponds, check dams, and gully plugs, are widely adopted by farmers in the cattle corridor to mitigate the unpredictable rainfall and recurrent droughts [22]. This study identified optimal locations for stormwater harvesting structures by evaluating key soil and water conservation factors, including slope, runoff depth, LULC, soil type, and stream order (Table 2) [44]. A suitability map was generated using an overlay analysis, where weighted overlay techniques were applied by assigning ranks and weights to each factor based on its influence [2,7,55]. This approach enabled the precise identification of ideal sites for effective stormwater harvesting structure.

Table 2. Criteria used to evaluate ideal structures by relative importance of each layer [2,7,55].

No.	Structure	Soil Texture	HSG	LULC	Slope	Runoff Potential	Stream Order
1.	Farm ponds	Sandy clay loam/Clay loam	B	Cropland	≤5	Moderate to high	1–4
(Influence by weight %)		(3)	(3)	(8)	(6)	(54)	(12)
2.	Check dams	Clay loam	C	Open water/stream	≤15	Moderate to high	1–4
(Influence by weight %)		(3)	(3)	(7)	(6)	(45)	(11)
3.	Gully plugging	Sandy clay loam/Clay	D	Drainage Channel	≥10	High	1–2
(Influence by weight %)		(7)	(7)	(7)	(35)	(37)	(7)

A weighted ranking system was implemented, assigning scores from 1 to 5 and weights ranging from 3 to 54, based on each factor's significance in stormwater harvesting [55]. Polygons meeting suitability criteria were given codes (0–6) to represent the suitable stormwater harvesting solutions, ensuring site-specific structures that optimize water conservation and system efficiency.

3. Results and Discussion

The integration of the SCS-CN method with spatial datasets in ArcGIS yielded significant results, pinpointing 80 ideal locations for stormwater interception in data-scarce regions to enhance stormwater storage and utilization. The assessment utilized key factors including soil texture, slope, HSG, LULC, CN, rainfall distribution, and runoff.

3.1. Soil Data

3.1.1. Soil Texture

Soil texture plays a crucial role in runoff by affecting water retention and infiltration, making it a key factor in optimizing stormwater harvesting sites. Clay soils, with low permeability and high water-holding capacity, are ideal for storage, while sandy soils promote rapid infiltration [56]. This study identified three main soil textures (Figure 7a):

sandy clay loam (91% of the area, 29,627 km²), loam (6%, 2031 km²), and clay loam (less than 1%, 39 km²). Sandy clay loam comprises 20–35% clay and 45–65% sand, offering a balanced mix of infiltration, retention, and drainage, making it highly suitable for stormwater harvesting [32,47]. Similarly, loam soils provide a favorable balance of water retention and erosion resistance [27]. The predominant soil characteristics in the study area highlight its strong potential for effective stormwater management.

3.1.2. Hydrological Soil Group

The HSG map (Figure 7b) identifies three groups: HSG B has the least coverage of 1720 km² (5%) in the south, HSG C spans 19,837 km² (61%) in the north and south, and HSG D covers 10,140 km² (31%) in the central region. HSG C and D demonstrate low infiltration and high-water retention, ideal for stormwater storage, although careful management of slope and drainage is required to prevent erosion due to their higher runoff potential [5,28,42,47]. In contrast, HSG B has moderate infiltration and lower runoff, more suited for groundwater recharge due to its balance between water infiltration and storage [33,51]. The spatial distribution of soil types significantly influences runoff generation, demonstrating their importance in stormwater analysis [33,42].

3.2. Land Use and Land Cover Map

The LULC map, derived from MODIS data, was simplified into five main categories: grassland (58%), cropland (39%), forest (1%), open water (1%), and minimal built-up areas (Figure 6). Grasslands and croplands dominate the region, underscoring the need for stormwater harvesting to enhance water availability for livestock and agriculture. LULC significantly influences precipitation–runoff dynamics, with vegetated areas like forests and grasslands promoting infiltration and reducing runoff coefficients [33,38]. In contrast, sparsely vegetated or impervious surfaces, such as urban areas, generate higher runoff [18]. Additionally, LULC distribution is critical for determining CN in hydrological models, directly affecting runoff estimates and supporting stormwater management strategies [33,38].

3.3. Curve Number

The CN map (Figure 9a) illustrates a pixel-wise CN range of 55 to 100, reflecting the influence of land use, soil texture, and hydrological conditions on rainfall–runoff dynamics. Low CN values (near 55), covering 5% of the area, are associated with forests and grasslands on loam or sandy loam soils (HSG A and B), which promote infiltration and are ideal for stormwater harvesting [39,47]. Moderate CN values (70–85), dominating 75% of the region, correspond to croplands with sandy clay loam soils (HSG B and C), offering a balance between runoff and infiltration [39,47]. High CN values (86–100), covering 20%, are linked to clay and clay loam soils (HSG C and D), bare lands, and impervious surfaces, indicating high runoff potential. This distribution emphasizes the need for integrated land and water management to reduce runoff, enhance infiltration, and optimize stormwater harvesting efforts across diverse landscapes [47].

3.4. Slope

A slope significantly influences water flow, runoff speed, and infiltration rates, making it a critical factor in evaluating stormwater harvesting potential [8,53]. In this study, slopes range from 0 to 67 degrees (Figure 10a) and are categorized into five groups: flat/gentle (0–5°), covering 60% of the area; gentle to moderate (5–10°), at 28%; moderate (10–15°), at 7%; steep (15–20°), at 3%; and very steep (>20°), at 2%. Most of the area (19,605 km² with flat slopes and 8974 km² with moderate slopes (0–10°)) is highly suitable for stormwater harvesting due to a balanced interaction between runoff and infiltration,

enabling effective water collection and retention [27,34]. In steeper areas, where runoff accelerates, infiltration decreases, and erosion risks increase, targeted measures such as erosion control and water diversion systems are necessary [1,32]. These systems direct runoff to flatter terrains, ensuring effective stormwater management across varying landscapes. This approach maximizes water capture while mitigating erosion in challenging topographies [32,34].

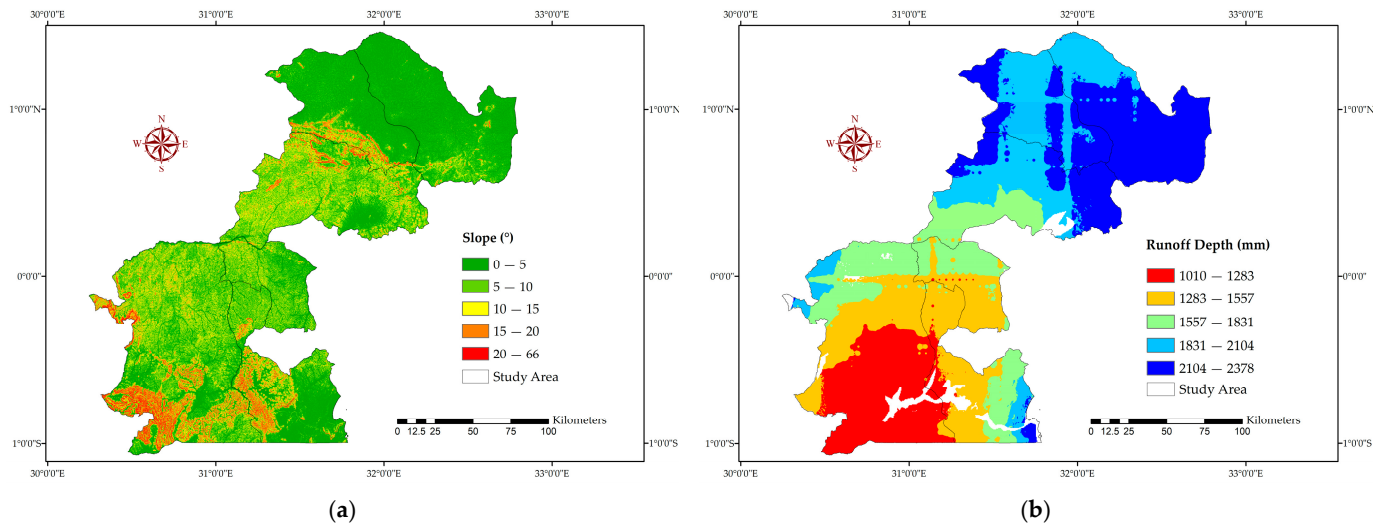


Figure 10. Variation in slope and runoff depth within the study area boundary: (a) slope map; (b) surface runoff depth map.

3.5. Rainfall Distribution

Using CHRS data from 2004 to 2023 [43], the study area receives an average annual rainfall of 1136 to 2448 mm (Figure 8), categorizing it as a moderate to high rainfall zone suitable for large-scale stormwater harvesting [47]. Rainfall distribution was classified into five categories to guide region-specific stormwater management strategies. The northern region, receiving the highest rainfall (1905–2448 mm annually) over 47% of the area, requires robust storage systems and efficient drainage to mitigate flooding and erosion risks. In contrast, the southern region, with lower rainfall (1136–1650 mm annually) covering 37% of the area, faces fewer risks but still benefits from effective runoff capture and storage practices. Understanding rainfall distribution is vital for designing tailored storage and drainage solutions that enhance water retention while minimizing runoff-related challenges.

3.6. Runoff Potential

The runoff depth map (Figure 10b) highlights the proportion of rainfall converting into surface runoff, a key factor in identifying ideal stormwater harvesting sites. Runoff potential closely mirrors rainfall distribution, reflecting the regions' response to precipitation and surface water availability for harvesting [49,53]. The runoff depth was divided into five categories: very high (2104–2378 mm) covering 15% in the northern area, moderately high (1831–2104 mm) covering 31%, high (1557–1831 mm) at 17%, moderate-low (1283–1557 mm) at 22%, and low (1010–1283 mm) at 15%. While the southern region (37% of the area) shows low runoff potential, the northern region (46%) experiences high runoff depths, increasing vulnerability to flooding and erosion. This emphasizes the need for region-specific strategies, particularly in the north, such as constructing large storage and runoff-trap structures to reduce risks and optimize water capture. The map provides

valuable insights into the watershed's hydrological response, guiding effective stormwater management interventions.

3.7. Watershed Delineation

This study defined 80 suitable small watersheds for stormwater harvesting using a gride code stream classification hierarchy (Figure 5a), with pour points (representing the highest flow accumulation) placed at the downstream ends of level 3 streams to define the contributing areas. This divided large basins into smaller, manageable units, facilitating the implementation of localized stormwater harvesting structures like farm ponds, check dams, and gully plugs. These targeted interventions enhance flood control, erosion prevention, groundwater recharge, and community involvement, boosting the effectiveness and resilience of stormwater management systems [27,39,52,56]. The methodology is highly adaptable, allowing pour point adjustments to accommodate watersheds of any size. This flexibility enables quick implementation of stormwater solutions without extensive analysis, reducing time and costs while maintaining precision. Integrating key site-selection factors and watershed-customized solutions fosters localized, efficient, and sustainable stormwater management strategies.

3.8. Potential Stormwater Harvesting Structures for the Demarcated Watershed

The structures' suitability map (Figure 11a) highlights regions ideal for farm ponds (0%), check dams (1%), gully plugs (1%), farm ponds and check dams (27%), and gully plugs and check dams (56%) based on the specific criteria (Table 2). The delineated watersheds, integrated with the suitability map, accurately align optimal stormwater harvesting structures with specific watershed conditions. This overlay (Figure 11a,b) enables the precise identification of suitable structures and provides estimates of potential water storage capacity at stipulated locations within the study area (Table A1). The estimated annual surface runoff volume across the 80 watershed spans from 62 to 557 million m³ (Table A1), representing a robust opportunity for stormwater harvesting to support irrigation, livestock, groundwater recharge, and community water supply in the study area. The structure suitability map (Figure 11b) reveals that 56 of the 80 watersheds (70%) are viable for multiple stormwater harvesting structures like farm ponds, check dams, or gully plugging. A total of 35 watersheds in the north can support about two structures due to favorable slopes, LULC, and runoff potential. However, 24 watersheds in the south are unsuitable for any intervention due to very steep slopes and low runoff.

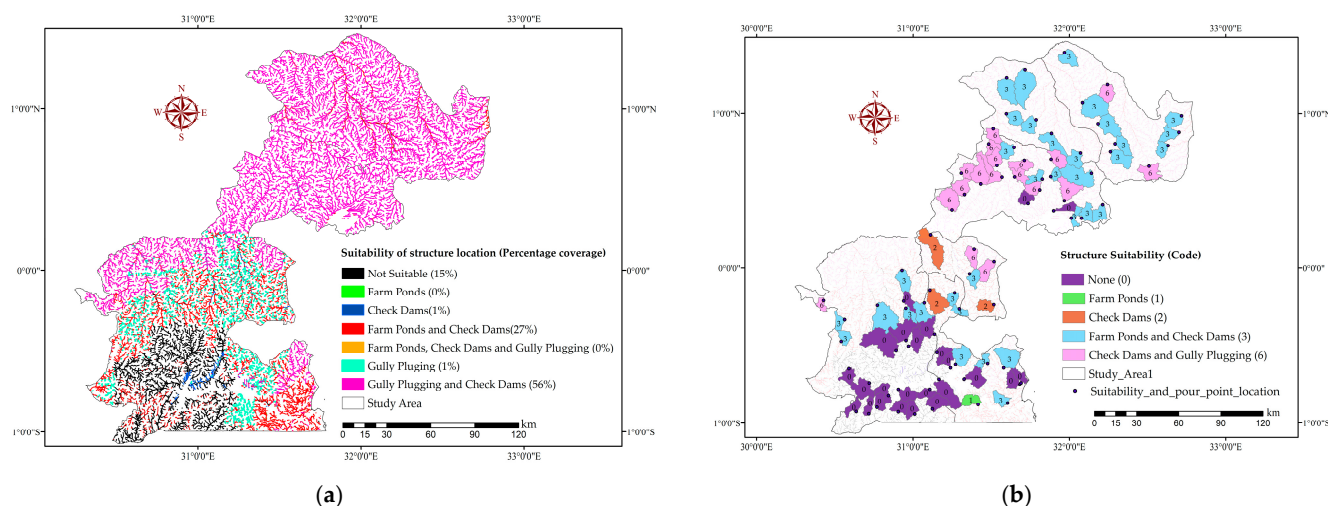


Figure 11. Suitable locations for stormwater harvesting structures: (a) structures' suitability map; (b) suitable structures for the demarcated watersheds.

Runoff volume estimates of each watershed promote customized structural designs that optimize water collection, ensure adequate storage, and incorporate erosion and flood control measures for high-risk areas [42,54]. They can also foster the enhancement of groundwater recharge to manage runoff and stabilize groundwater levels in areas not suitable for any intervention [57]. Watershed-specific runoff volumes are critical for water resource planning, informing the placement of stormwater storage structures that also aid in flood control and environmental impact reduction.

This study provides crucial data to support informed decision-making for water resource authorities and farmers, enabling efficient resource allocation and the design of adaptable stormwater harvesting structures. By addressing climate-induced water shortages, the approach enhances agricultural productivity and resilience. The weighted overlay method ensures precise stormwater management by tailoring solutions to specific watershed conditions, making it both practical and scalable. Additionally, the study delivers significant social, economic, and environmental benefits, including improved water availability for agriculture and livestock, reduced water scarcity, and long-term sustainability [5,14,18,35].

The findings align with global advancements in GIS-based stormwater harvesting [2,8,18]. Unlike large-scale basin-wide assessments in urban settings, this study focuses on smaller watersheds in semi-arid rural regions, demonstrating the adaptability of GIS-based methods across different landscapes [18]. Compared to [8] who developed a GIS-based framework for rainwater harvesting site selection, this study refines the methodology by incorporating weighted overlay, refining site selection for data-scarce environments, tailoring solutions specifically to Uganda's cattle corridor, and multiple selection criteria such as soil texture, stream order, and land use, ensuring a more comprehensive and location-specific assessment.

By pioneering a GIS-driven stormwater harvesting approach in Uganda's cattle corridor, this research provides a practical tool for managing water resources in data-scarce regions, contributing to rural development, food security, and climate resilience. While socio-economic factors and structural design elements were beyond the study's scope, they are acknowledged as influential for site suitability and are recommended for future research [51], alongside the validation of these results, to further optimize this methodology. Ultimately, the comprehensive runoff volume data are an asset for urban and regional planning, supporting policies to reduce runoff, enhance water retention, and conserve natural landscapes, while alleviating stormwater impacts on the hydrological cycle [42,54].

The plot of runoff depth, area, and volume (Figure 12a), shows a strong correlation (0.91) between watershed area and runoff volume (Figure 12b), whereas the correlation between runoff depth and volume (0.41) is moderate, indicating a significant influence of factors like slope, soil type, and LULC on runoff volume beyond just depth. An analysis using the Google Earth Engine revealed that the identified stormwater harvesting sites are strategically located near key water features, including farm ponds, swamps, rivers, lakes, and open land (Table A1). These insights are crucial for prioritizing and selecting the most suitable water storage structures based on site-specific conditions, enhancing the effectiveness of stormwater management

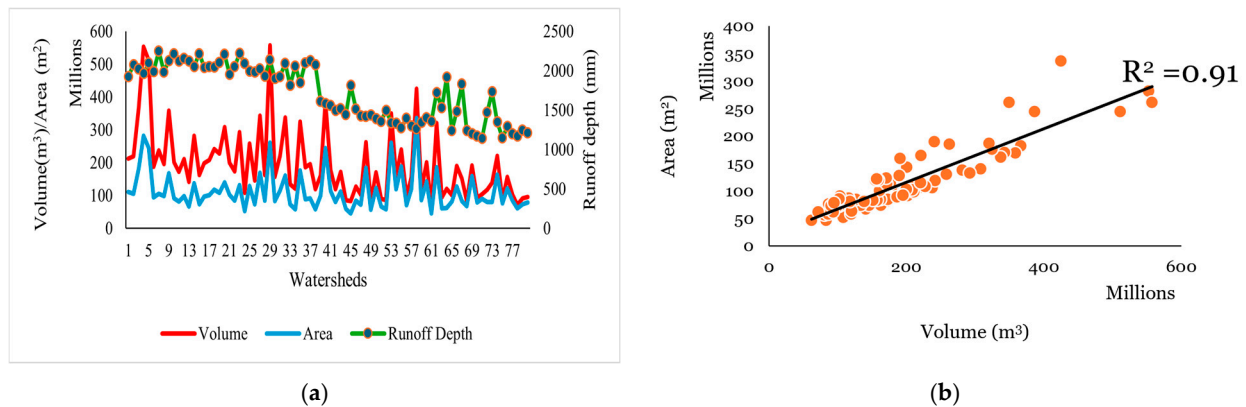


Figure 12. Correlation between runoff volume, watershed area, and runoff depth: (a) a plot of the watershed area, runoff volume, and depth; (b) strong positive correlation between watershed area and runoff volume.

4. Conclusions

Uganda's cattle corridor faces critical water scarcity and unpredictable rainfall, emphasizing the need for sustainable stormwater harvesting solutions. This study employed a GIS-based approach combined with the SCS-CN method to assess runoff potential and identify optimal locations for water storage structures. Of the 80 delineated watersheds, 56 (70%) were deemed suitable for structures such as farm ponds, check dams, and gully plugs. These interventions can significantly enhance water availability, supplementing conventional sources that often dry up during prolonged droughts, thereby improving water security for livestock and irrigation.

Suitability was determined by evaluating key hydrological and landscape factors, including runoff potential, slope, soil texture, LULC, HSG, and stream order. The study estimated annual runoff volumes ranging from 62 million cubic meters in small watersheds to 557 million cubic meters in larger ones. By aligning structure selection with local conditions, this approach optimizes stormwater capture and storage, supporting resilient agricultural practices and sustainable water resource management.

This study pioneers the application of a GIS-based stormwater harvesting approach in Uganda's cattle corridor, offering a practical and data-driven tool for water resource management in data-scarce regions. By integrating weighted overlay and Boolean analysis, the methodology enhances site selection accuracy, maximizing stormwater capture for sustainable use. The findings provide actionable solutions to improve water availability while delivering significant social, economic, and environmental benefits. These contributions support rural development, strengthen food security, and enhance climate resilience, directly impacting local communities by offering solutions tailored to their specific needs and challenges. The study also offers valuable guidance for policymakers and farmers in optimizing resource allocation and infrastructure planning. Future research is recommended on validating runoff estimates through field measurements or employing remote sensing data on soil water accumulation and refining the approach to account for seasonal variations, ensuring broader applicability across diverse agro-ecological zones.

Author Contributions: Conceptualization, methodology, software, writing, G.S.; review and editing, M.J.A. and K.-S.C.; administration and supervision, K.-S.C. All authors have read and agreed to the published version of the manuscript.

Funding: This research received no funding.

Data Availability Statement: The raw data used in this study can be accessed from the different data platforms cited in the article.

Acknowledgments: We extend our gratitude to the Institute of International Research and Development at Kyungpook National University through the Korea International Cooperation Agency (KOICA) Scholarship Program for Sponsoring Creative Global Leaders. We appreciate their support and guidance for this scholarship program.

Conflicts of Interest: The authors declare no conflicts of interest.

Appendix A

Table A1. Optimal stormwater harvesting sites' locations, recommended harvesting structures (codes), and estimated runoff volume.

Watershed No.	Area (km ²)	Mean Runoff Depth (mm)	Runoff Volume (hm ³)	Longitude (°)	Latitude (°)	Suitability Code	Observation (Google Earth)
1	110.7	1924	212.9	31.9683	1.3978	3	Open land
2	105.3	2077	218.7	32.2433	1.1881	6	Near ponds
3	181.2	2023	366.6	31.5983	1.2306	3	Open land
4	281.5	1963	552.7	31.7161	1.2864	3	Open land
5	243.7	2099	511.6	32.0836	1.0719	3	Near River
6	94.3	1990	187.7	31.5967	0.9989	3	Near Pond
7	105.8	2247	237.8	32.7169	0.9858	3	Open land
8	98.8	1984	196.1	31.7867	0.9594	3	Near Pond
9	168.4	2131	358.9	32.1833	0.9342	3	Near Lake
10	91.1	2215	201.8	32.7006	0.8786	3	Open land
11	81.2	2124	172.4	31.5131	0.9008	6	Open land
12	97.9	2155	211.1	32.2922	0.8075	3	Open land
13	66.5	2123	141.2	31.4839	0.8058	6	Swamp
14	137.1	2055	281.7	31.8856	0.8714	3	Open land
15	73.5	2216	162.8	32.6311	0.7953	3	Open land
16	96.9	2043	198.1	31.6456	0.7833	3	Open land
17	101.4	2054	208.3	31.5364	0.6642	6	Swamp
18	118.3	2046	241.9	31.8825	0.7056	6	Swamp
19	108.0	2107	227.6	32.0711	0.7469	3	Open land
20	139.5	2208	308.0	32.2628	0.7553	3	Open land
21	102.4	1955	200.1	31.7114	0.6981	6	Open land
22	84.3	2053	173.0	31.3089	0.6136	6	Swamp
23	131.8	2221	292.7	32.5089	0.6600	6	Swamp
24	51.6	2095	108.2	31.8808	0.5917	3	Near Swamp
25	129.5	1994	258.2	31.5689	0.5883	6	Swamp
26	73.7	1983	146.0	31.8269	0.5753	3	Near Pond
27	169.4	2022	342.6	31.4331	0.5408	6	Swamp
28	84.2	1929	162.3	31.6497	0.5892	6	Open land
29	260.5	2140	557.4	32.1408	0.6133	3	Swamp
30	82.8	1901	157.3	31.8100	0.5033	6	Near ponds
31	114.4	1928	220.5	31.3289	0.4758	6	Open land
32	161.2	2095	337.6	31.9675	0.4367	6	Swamp
33	73.8	1814	133.9	31.7358	0.4181	0	Open land
34	58.4	2060	120.2	31.8994	0.3703	0	Lake Wamala
35	175.8	1848	324.9	31.2492	0.3761	6	Near Swamp
36	88.8	2100	186.5	32.0778	0.3217	3	Swamp
37	91.8	2126	195.1	32.2125	0.4100	3	Swamp
38	57.7	2074	119.7	32.0119	0.3225	3	Swamp
39	99.8	1613	161.1	31.3908	0.1236	6	Open land
40	243.9	1585	386.6	31.1125	0.2175	2	Near River

41	113.4	1561	177.0	31.5178	0.0397	6	Near Gully
42	80.1	1494	119.7	31.3614	-0.0400	3	Open land
43	112.5	1522	171.3	30.9294	-0.0169	3	Near Ponds
44	58.9	1443	85.0	31.2661	-0.1603	3	Near Ponds
45	45.8	1816	83.3	30.4283	-0.2097	6	Open land
46	83.9	1514	127.0	31.5169	-0.2364	2	Open land
47	71.7	1424	102.1	30.9408	-0.2131	0	Open land
48	184.4	1424	262.5	31.1072	-0.1428	2	Near Ponds
49	56.1	1438	80.6	31.2964	-0.2631	3	Open land
50	122.9	1390	170.9	31.0728	-0.2244	3	Open land
51	66.0	1357	89.6	30.9542	-0.2603	3	Open land
52	57.5	1498	86.2	30.5631	-0.3336	3	Swamp
53	261.0	1340	349.7	30.7722	-0.2408	3	Open land
54	119.3	1335	159.3	31.1378	-0.4286	0	Open land
55	188.8	1275	240.8	30.9556	-0.4683	0	Open land
56	70.1	1400	98.2	30.5408	-0.4744	3	Open land
57	119.2	1300	155.0	30.9711	-0.5058	0	Near River
58	335.9	1265	424.8	30.8922	-0.5361	0	Open land
59	86.2	1348	116.2	31.1528	-0.5469	0	Near Lake
60	142.8	1405	200.6	31.2714	-0.6247	3	Waterbody
61	45.8	1360	62.2	31.2392	-0.6492	0	Waterbody
62	185.9	1724	320.5	31.5797	-0.6492	3	Open land
63	61.2	1528	93.6	31.4767	-0.6197	3	Open land
64	62.7	1917	120.1	31.6906	-0.7433	0	Open land
65	81.9	1239	101.5	30.5906	-0.6542	0	Open land
66	127.8	1485	189.9	31.3261	-0.7194	0	Lake
67	82.5	1833	151.2	31.6831	-0.7542	0	Near Lake
68	67.0	1239	83.0	31.1067	-0.7881	0	Open land
69	158.9	1202	191.0	30.7211	-0.7433	0	Open land
70	78.7	1172	92.2	30.9064	-0.7878	0	Lake
71	90.5	1143	103.5	30.8431	-0.8256	0	Lake
72	80.1	1471	117.8	31.4161	-0.8847	1	Open land
73	80.0	1734	138.7	31.6050	-0.8761	3	Open land
74	163.9	1350	221.3	31.1658	-0.7197	0	Lake
75	75.8	1146	86.9	30.7689	-0.9017	0	Open land
76	121.2	1292	156.6	31.1236	-0.9125	0	Open land
77	84.9	1202	102.0	30.9056	-0.9297	0	Open land
78	61.2	1172	71.7	30.7172	-0.9425	0	Open land
79	72.7	1248	90.7	30.6364	-0.9286	0	Open land
80	78.4	1211	94.9	31.0111	-0.9444	3	Waterbody

Notes: Suitability codes assigned to the different polygons include 0 (None of the structure), 1 (Farm Ponds), 2 (Check Dams), 3 (Farm Ponds and Check Dams), 6 (Check Dams and Gully Plugging).

References

1. Manaouch, M.; Sadiki, M.; Fenjiro, I. Integrating GIS-based FAHP and WaTEM/SEDEM for identifying potential RWH areas in semi-arid areas. *Geocarto Int.* **2021**, *37*, 8882–8905. <https://doi.org/10.1080/10106049.2021.2007295>.
2. Kumar, T.; Jhariya, D.C. Identification of rainwater harvesting sites using SCS-CN methodology, remote sensing and Geographical Information System techniques. *Geocarto Int.* **2016**, *32*, 1367–1388. <https://doi.org/10.1080/10106049.2016.1213772>.
3. Liu, J.; Yang, H.; Gosling, S.N.; Kummu, M.; Florke, M.; Pfister, S.; Hanasaki, N.; Wada, Y.; Zhang, X.; Zheng, C.; et al. Water scarcity assessments in the past, present and future. *Earths Future* **2017**, *5*, 545–559. <https://doi.org/10.1002/2016EF000518>.

4. Hussain, A.; Rahman, K.U.; Shahid, M.; Haider, S.; Pham, Q.B.; Linh, N.T.T.; Sammen, S.S. Investigating feasible sites for multi-purpose small dams in Swat District of Khyber Pakhtunkhwa Province, Pakistan: Socioeconomic and environmental considerations. *Environ. Dev. Sustain.* **2021**, *24*, 10852–10875. <https://doi.org/10.1007/s10668-021-01886-z>.
5. Asmar, N.F.; Sim, J.O.L.; Ghodieh, A.; Fauzi, R. Effect of Land Use\Land Cover Changes on Estimated Potential Runoff in the Nablus Mountains Watersheds of Palestine: A Case Study. *J. Indian Soc. Remote Sens.* **2021**, *49*, 1067–1080. <https://doi.org/10.1007/s12524-020-01278-2>.
6. Jafari Shalamzari, M.; Zhang, W.; Gholami, A.; Zhang, Z. Runoff Harvesting Site Suitability Analysis for Wildlife in Sub-Desert Regions. *Water* **2019**, *11*, 1944. <https://doi.org/10.3390/w11091944>.
7. Kolekar, S.S.; Mishra, A.; Choudhari, P.; Choudhari, N.R. Identification of specific areas for water conservation measures using Geoinformatics approach. *Arab. J. Geosci.* **2021**, *14*, 1–13. <https://doi.org/10.1007/s12517-021-06721-3>.
8. Tiwari, K.; Goyal, R.; Sarkar, A. GIS-based Methodology for Identification of Suitable Locations for Rainwater Harvesting Structures. *Water Resour. Manag.* **2018**, *32*, 1811–1825. <https://doi.org/10.1007/s11269-018-1905-9>.
9. Zabidi, H.A.; Goh, H.W.; Chang, C.K.; Chan, N.W.; Zakaria, N.A. A Review of Roof and Pond Rainwater Harvesting Systems for Water Security: The Design, Performance and Way Forward. *Water* **2020**, *12*, 3163. <https://doi.org/10.3390/w12113163>.
10. Raimondi, A.; Quinn, R.; Abhijith, G.R.; Becciu, G.; Ostfeld, A. Rainwater Harvesting and Treatment: State of the Art and Perspectives. *Water* **2023**, *15*, 1518. <https://doi.org/10.3390/w15081518>.
11. Teston, A.; Geraldi, M.; Colasio, B.; Ghisi, E. Rainwater Harvesting in Buildings in Brazil: A Literature Review. *Water* **2018**, *10*, 471. <https://doi.org/10.3390/w10040471>.
12. Teston, A.; Piccinini Scolaro, T.; Kuntz Maykot, J.; Ghisi, E. Comprehensive Environmental Assessment of Rainwater Harvesting Systems: A Literature Review. *Water* **2022**, *14*, 2716. <https://doi.org/10.3390/w14172716>.
13. Melville-Shreeve, P.; Ward, S.; Butler, D. A preliminary sustainability assessment of innovative rainwater harvesting for residential properties in UK. *J. Southeast Univ.* **2014**, *30*, 135–142.
14. Aghad, M.; Manaouch, M.; Sadiki, M.; Batchi, M.; Al Karkouri, J. Identifying Suitable Sites for Rainwater Harvesting Using Runoff Model (Scs-Cn), Remote Sensing and Gis Based Fuzzy Analytical Hierarchy Process (Fahp) in Kenitra Province, Nw Morocco. *Geogr. Tech.* **2021**, *16*, 111–127. https://doi.org/10.21163/gt_2021.163.09.
15. Doulabian, S.; Ghasemi Tousi, E.; Aghlmand, R.; Alizadeh, B.; Ghaderi Bafti, A.; Abbasi, A. Evaluation of Integrating SWAT Model into a Multi-Criteria Decision Analysis towards Reliable Rainwater Harvesting Systems. *Water* **2021**, *13*, 1935. <https://doi.org/10.3390/w13141935>.
16. Sayl, K.N.; Mohammed, A.S.; Ahmed, A.D. GIS-based approach for rainwater harvesting site selection. *IOP Conf. Ser. Mater. Sci. Eng.* **2020**, *737*, 012246. <https://doi.org/10.1088/1757-899x/737/1/012246>.
17. Preeti, P.; Shendryk, Y.; Rahman, A. Identification of Suitable Sites Using GIS for Rainwater Harvesting Structures to Meet Irrigation Demand. *Water* **2022**, *14*, 3480. <https://doi.org/10.3390/w14213480>.
18. Patil, D.; Kumar, G.; Kumar, A.; Gupta, R. A systematic basin-wide approach for locating and assessing volumetric potential of rainwater harvesting sites in the urban area. *Env. Sci. Pollut. Res. Int.* **2023**, *30*, 14707–14721. <https://doi.org/10.1007/s11356-022-23039-z> From NLM Medline.
19. Fassman-Beck, E.; Schiff, K.; Apt, D. *Evaluating Potential Methods to Quantify Stormwater Capture*; SCCWRP Technical Report 1116; SCCWRP: Costa Mesa, CA, USA, 2020.
20. Nansamba, M.; Sibiya, J.; Tumuhimbise, R.; Ocimati, W.; Kikulwe, E.; Karamura, D.; Karamura, E. Assessing drought effects on banana production and on-farm coping strategies by farmers—A study in the cattle corridor of Uganda. *Clim. Change* **2022**, *173*, 1–20. <https://doi.org/10.1007/s10584-022-03408-w>.
21. Mayanja, M.N.; Rubaire-Akiiki, C.; Morton, J.; Kabasa, J.D. Pastoral community coping and adaptation strategies to manage household food insecurity consequent to climatic hazards in the cattle corridor of Uganda. *Clim. Dev.* **2019**, *12*, 110–119. <https://doi.org/10.1080/17565529.2019.1605283>.
22. Kiggundu, N.; Wanyama, J.; Mfitumukiza, D.; Twinomuhangi, R.; Barasa, B.; Katimbo, A.; Birungi Kyazze, F. Rainwater harvesting knowledge and practice for agricultural production in a changing climate: A review from Uganda’s perspective. *Agric. Eng. Int. CIGR J.* **2018**, *20*, 19–36.
23. Nanfuka, S.; Mfitumukiza, D.; Egeru, A. Characterisation of ecosystem-based adaptations to drought in the central cattle corridor of Uganda. *Afr. J. Range Forage Sci.* **2020**, *37*, 257–267. <https://doi.org/10.2989/10220119.2020.1748713>.
24. Nalwanga, F.S.; Nanteza, J.; Obua, J.; Nimusiima, A.; Mukwaya, P.; Kitembe, J.; Odongo, R.; Musali, P.; Nabanoga, G.N.; Kisira, Y. Insights into meteorological drought: Navigating Uganda’s cattle corridor through past trends and future projections. *Nat. Hazards* **2024**, *120*, 8695–8721. <https://doi.org/10.1007/s11069-024-06545-w>.

25. Mbaziira, J. Insights into agropastoral communities' innovations in Uganda's cattle corridor. *Sustain. Technol. Entrep.* **2023**, *2*, 100038. <https://doi.org/10.1016/j.stae.2023.100038>.
26. Ingraio, C.; Strippoli, R.; Lagioia, G.; Huisingh, D. Water scarcity in agriculture: An overview of causes, impacts and approaches for reducing the risks. *Heliyon* **2023**, *9*, e18507. <https://doi.org/10.1016/j.heliyon.2023.e18507>.
27. Gavhane, K.P.; Mishra, A.K.; Sarangi, A.; Singh, D.K.; Sudhishri, S. Targeting of rainwater harvesting structures using geospatial tools and analytical hierarchy process (AHP) in the semi-arid region of Rajasthan (India). *Environ. Sci. Pollut. Res.* **2023**, *30*, 61682–61709. <https://doi.org/10.1007/s11356-023-26289-7>.
28. Gebremedhn, A.Y.; Getahun, Y.S.; Moges, A.S.; Tesfay, F. Identification of Suitable Rainwater Harvesting Sites Using Geospatial Techniques With AHP in Chacha Watershed, Jemma Sub-Basin Upper Blue Nile, Ethiopia. *Air Soil Water Res.* **2023**, *16*, 1–16. <https://doi.org/10.1177/11786221231195831>.
29. Fatumah, N.; Mohammed, S.; Ashraf, N.; Abasi, K.; Shadia, N. Adoption of novel climate-smart farming systems for enhanced carbon stock and carbon dioxide equivalent emission reduction in cattle corridor areas of Uganda. *Heliyon* **2023**, *9*, e14114. <https://doi.org/10.1016/j.heliyon.2023.e14114>.
30. Nanyeenya, N.W.; Bugeza, J.; Kigozi, A.; Kayiwa, S.; Sserumaga, P.; Semwanga, M.; Segawa, A.; Nakiguli, F.; Zziwa, E.; Kabanda, N.; et al. Understanding the dynamics of access to water for beef production and adoption of valley tanks in eight cattle corridor districts of Uganda. *RUFORUM Work. Doc. Ser.* **2022**, *20*, 10–18.
31. Al-Ghobari, H.; Dewidar, A.Z. Integrating GIS-Based MCDA Techniques and the SCS-CN Method for Identifying Potential Zones for Rainwater Harvesting in a Semi-Arid Area. *Water* **2021**, *13*, 704. <https://doi.org/10.3390/w13050704>.
32. Kadam, A.K.; Kale, S.S.; Pande, N.N.; Pawar, N.J.; Sankhua, R.N. Identifying Potential Rainwater Harvesting Sites of a Semi-arid, Basaltic Region of Western India, Using SCS-CN Method. *Water Resour. Manag.* **2012**, *26*, 2537–2554. <https://doi.org/10.1007/s11269-012-0031-3>.
33. Naidu, K.; Ramlal, S.; Rao, V. Runoff Estimation of Mini Watershed of Pedda Kedari Reserve Forest, Tekkali, Srikakulam, AP Using Remote Sensing, GIS And SCS Curve Number Techniques. *Int. J. Civ. Eng. Technol. (IJCIET)* **2019**, *10*, 1999–2013.
34. Rajasekhar, M.; Gadhiraaju, S.R.; Kadam, A.; Bhagat, V. Identification of groundwater recharge-based potential rainwater harvesting sites for sustainable development of a semiarid region of southern India using geospatial, AHP, and SCS-CN approach. *Arab. J. Geosci.* **2020**, *13*, 24. <https://doi.org/10.1007/s12517-019-4996-6>.
35. Al-Khuzai, M.M.; Janna, H.; Al-Ansari, N. Assessment model of water harvesting and storage location using GIS and remote sensing in Al-Qadisiyah, Iraq. *Arab. J. Geosci.* **2020**, *13*, 1–9. <https://doi.org/10.1007/s12517-020-06154-4>.
36. Shadmehri Toosi, A.; Ghasemi Tousi, E.; Ghassemi, S.A.; Cheshomi, A.; Alaghmand, S. A multi-criteria decision analysis approach towards efficient rainwater harvesting. *J. Hydrol.* **2020**, *582*, 124501. <https://doi.org/10.1016/j.jhydrol.2019.124501>.
37. Zhang, S.; Li, Y.; Ma, M.; Song, T.; Song, R. Storm Water Management and Flood Control in Sponge City Construction of Beijing. *Water* **2018**, *10*, 1040. <https://doi.org/10.3390/w10081040>.
38. Napoli, M.; Cecchi, S.; Orlandini, S.; Zanchi, C.A. Determining potential rainwater harvesting sites using a continuous runoff potential accounting procedure and GIS techniques in central Italy. *Agric. Water Manag.* **2014**, *141*, 55–65. <https://doi.org/10.1016/j.agwat.2014.04.012>.
39. Zhong, S.; Liu, W.; Ni, C.; Yang, Q.; Ni, J.; Wei, C. Runoff harvesting engineering and its effects on soil nitrogen and phosphorus conservation in the Sichuan Hilly Basin of China. *Agric. Ecosyst. Environ.* **2020**, *301*, 107022. <https://doi.org/10.1016/j.agee.2020.107022>.
40. Sujud, L.H.; Jaafar, H.H. A global dynamic runoff application and dataset based on the assimilation of GPM, SMAP, and GCN250 curve number datasets. *Sci. Data* **2022**, *9*, 1–11. <https://doi.org/10.1038/s41597-022-01834-0>.
41. Uganda Bureau of Statistics, U. National Population and Housing Census 2024—Preliminary Results; Kampala, Uganda, 2024.
42. Radwan, F.; Alazba, A.A.; Mossad, A. Estimating potential direct runoff for ungauged urban watersheds based on RST and GIS. *Arab. J. Geosci.* **2018**, *11*, 748. <https://doi.org/10.1007/s12517-018-4067-4>.
43. Nguyen, P.; Shearer, E.J.; Tran, H.; Ombadi, M.; Hayatbini, N.; Palacios, T.; Huynh, P.; Braithwaite, D.; Updegraff, G.; Hsu, K.; et al. The CHRS Data Portal, an easily accessible public repository for PERSIANN global satellite precipitation data. *Sci. Data* **2019**, *6*, 180296. <https://doi.org/10.1038/sdata.2018.296>.
44. Soil Conservation Services United States. *SCS National Engineering Handbook, Section 4: Hydrology*; US 444 Department of Agriculture, US Government Printing Office: Washington, DC, USA, 1972.
45. Farooq, S.; Mahmood, K.; Faizi, F. Comparative Simulation of GIS-Based Rainwater Management Solutions. *Water Resour. Manag.* **2022**, *36*, 3049–3065. <https://doi.org/10.1007/s11269-022-03185-2>.

46. Mahmood, K.; Qaiser, A.; Farooq, S.; Nisa, M. u. RS- and GIS-based modeling for optimum site selection in rain water harvesting system: An SCS-CN approach. *Acta Geophys.* **2020**, *68*, 1175–1185. <https://doi.org/10.1007/s11600-020-00460-x>.
47. Mugo, G.M.; Odera, P.A. Site selection for rainwater harvesting structures in Kiambu County-Kenya. *Egypt. J. Remote Sens. Space Sci.* **2019**, *22*, 155–164. <https://doi.org/10.1016/j.ejrs.2018.05.003>.
48. Khan, D.; Raziq, A.; Young, H.-W.V.; Sardar, T.; Liou, Y.-A. Identifying Potential Sites for Rainwater Harvesting Structures in Ghazi Tehsil, Khyber Pakhtunkhwa, Pakistan, Using Geospatial Approach. *Remote Sens.* **2022**, *14*, 5008. <https://doi.org/10.3390/rs14195008>.
49. Ibrahim, G.R.F.; Rasul, A.; Ali Hamid, A.; Ali, Z.F.; Dewana, A.A. Suitable Site Selection for Rainwater Harvesting and Storage Case Study Using Dohuk Governorate. *Water* **2019**, *11*, 864. <https://doi.org/10.3390/w11040864>.
50. Asif, M.; Yaseen, M.; Shahid, S.U.; Latif, Y.; Anwar, S.; Abbas, S. Geospatial identification of possible rainwater harvesting locations within a high-altitude Gilgit River basin, Pakistan. *Theor. Appl. Climatol.* **2024**, *155*, 7991–8004. <https://doi.org/10.1007/s00704-024-05024-3>.
51. Pandey, P.; Tiwari, S.K.; Pandey, H.K.; Chaurasia, A.K.; Singh, S. Identification of Potential Recharge Zones in Drought Prone Area of Bundelkhand Region, India, Using SCS-CN and MIF Technique Under GIS-frame work. *Water Conserv. Sci. Eng.* **2021**, *6*, 105–125. <https://doi.org/10.1007/s41101-021-00105-0>.
52. Pathak, S.; Ojha, C.; Zevenbergen, C.; Garg, R. Ranking of Storm Water Harvesting Sites Using Heuristic and Non-Heuristic Weighing Approaches. *Water* **2017**, *9*, 710. <https://doi.org/10.3390/w9090710>.
53. Singhai, A.; Das, S.; Kadam, A.K.; Shukla, J.P.; Bundela, D.S.; Kalashetty, M. GIS-based multi-criteria approach for identification of rainwater harvesting zones in upper Betwa sub-basin of Madhya Pradesh, India. *Environ. Dev. Sustain.* **2017**, *21*, 777–797. <https://doi.org/10.1007/s10668-017-0060-4>.
54. MAmin, H.N.; Majeed, S.A. Runoff Estimation and Dam Selection Site in the Khur khur Watershed (KHW), Using (SCS-CN) Method and (GIS & RS) Techniques. *IOP Conf. Ser. Earth Environ. Sci.* **2022**, *1120*, 012019. <https://doi.org/10.1088/1755-1315/1120/1/012019>.
55. Aklan, M.; Al-Komaim, M.; de Fraiture, C. Site suitability analysis of indigenous rainwater harvesting systems in arid and data-poor environments: A case study of Sana'a Basin, Yemen. *Environ. Dev. Sustain.* **2022**, *25*, 8319–8342. <https://doi.org/10.1007/s10668-022-02402-7>.
56. Rejani, R.; Rao, K.V.; Srinivasa Rao, C.H.; Osman, M.; Sammi Reddy, K.; George, B.; Pratyusha Kranthi, G.S.; Chary, G.R.; Swamy, M.V.; Rao, P.J. Identification of Potential Rainwater-Harvesting Sites for the Sustainable Management of a Semi-Arid Watershed. *Irrig. Drain.* **2017**, *66*, 227–237. <https://doi.org/10.1002/ird.2101>.
57. Dangwal, A.; Sharma, A. Mitigation of Urban Flooding using Blue-Green Infrastructure: A Case of Dehradun City, India. *Disaster Adv.* **2022**, *15*, 50–61. <https://doi.org/10.25303/1511da050061>.

Disclaimer/Publisher's Note: The statements, opinions and data contained in all publications are solely those of the individual author(s) and contributor(s) and not of MDPI and/or the editor(s). MDPI and/or the editor(s) disclaim responsibility for any injury to people or property resulting from any ideas, methods, instructions or products referred to in the content.